Iranian Journal of Medical Physics

ijmp.mums.ac.ir

Synthesis of Colloidal Silver, Platinum, and Mixture of Silver-Platinum Nanoparticles Using Pulsed Laser Ablation as a Contrast Agent in Computed Tomography

Ali Khumaeni[1*], Mohammad Zamakhsari Alhamid[1], Choirul Anam[1], Ari Budiono[2]

1. Physics Department, Diponegoro University, Tembalang, Semarang, Central Java, Indonesia
2. Loekmono HadiGeneral Hospital,Kudus, Central Java, Indonesia

ARTICLE INFO

Article type:
Original Paper

Article history:
Received: Sep 06, 2020
Accepted: Jan 28, 2021

Keywords:
Diagnosis
Metal Nanoparticles
Contrast Agent
CT Scan

ABSTRACT

Introduction: The development of nanoparticles as computed tomography contrast agents has increased significantly. However, few reports have been published on the use of silver and platinum nanoparticles as contrast agents. These nanomaterials are a good candidatefor contrast agents because of their high atomic number and high durability against corrosion.
Material and Methods: Experimentally, a Nd:YAG laser (1064 nm, 45 mJ, 10 Hz) was focused on a high-purity metal plate including Ag and Pt plates, which are placed in deionized water medium. Colloidal nanoparticles of Ag and Pt were then mixed to obtain a mixture composition of Ag and Pt with ratios of Ag:Pt of 75:25%, 50:50%, 25:75%, respectively.The Ag, Pt, and Ag-Pt NPs mixture were then examined as contrast agents in CT scan.
Results: The imaging results of the quantitative analysiswere measured in the Hounsfield Unit(HU), showing 13.5, 12.8, 13.3, 14.1, and 17.3 HU for colloidal 100% AgNPs, colloidal Ag and Pt NPs with volume ratios of Ag:Pt of 75:25%, 50:50%, 25:75%, and colloidal 100%Pt NPs, respectively.
Conclusion: Results reveal the highest absorbent power was found in the colloidal contrast agent of Pt NPs 100% is 17.3 HU, followed by the 25:75% Ag-Pt NPs is 14.1 HU. The higher HU value for platinum can be attributed to its higher density since the effective energy of 80 kVp is about 42 keV, which is lower than the K-edge of Pt (K-edge ≈ 78 keV), which means that the attenuation of X-ray in Pt is due to Compton scattering dominantly.

►*Please cite this article as:*
Khumaeni A, Alhamid MZ, Anam Ch, Budiono A. Synthesis of Colloidal Silver, Platinum, and Mixture of Silver-Platinum Nanoparticles Using Pulsed Laser Ablation as a Contrast Agent in Computed Tomography. Iran J Med Phys 2022; 19: 49-57. 10.22038/IJMP.2021.51781.1849

Introduction

Early diagnosis of diseases is urgently imperative to prevent and screen the diseases in the human body. Various techniques have been commercially established to perform diagnosis of disease; one of them is visible spectrometry, which is commonly used for chronic diagnosis [1]. The other technique is x-ray based imaging technique, which is recently employed as a diagnostic technique of cancer in the human body.

Imaging technique based on X-ray has been employed in the medical field [2], Computed Tomography (CT) has been superior in terms of imaging and cost efficiencies and yet non-optimal in soft tissues detection. In this regard, attempts to enhance CT diagnostic qualities have used clinically standard contrast agents, such as the small molecular iodinated agent and barium suspension. These have only led to other essential problems in the medical imaging's, including high osmolality, contrast agent's low longevity, kidneys toxicity, and poor contrasts in patients with large body volumes [3]. Over the last seven years, the development of nanoparticles as CT'scontrast agents has increased significantly. Nanoparticles have several advantages compared to the micro-sized, molecular contrast agents, such as lower osmolality, longer longevity, potentials for cell tracking and targeted imaging applications [2]. Also, compared to iodine that is commonly employed as a contrast agent in CT scans, the absorption of nanoparticles is much higher with low tissue and bone interference, resulting in better contrast. Furthermore, the nanoparticles have a longer circulation time in the blood than the iodine case, yielding longer imaging times [3]. Metal nanoparticles are intensively exploited as a future candidate of contrast agent in CT scan because (a) their wide surface can be modified with the much more targeting molecules; (b) their plasma dissemination time can be turned north of a few significant degrees dependent on their physicochemical properties; and (c) drugs and contrast agent can be incorporated at foreordained proportions either in the inside or on the surfaces.

*Corresponding Author: Tel: +6281275397831; Email: khumaeni@fisika.fsm.undip.ac.id

The syntheses of metal nanoparticlesare generally achieved either chemically or physically. A typical, chemical process begins with the thermal decomposition of precursors into atoms, followed by aggregation into nanoparticles [4]. During this process, additives like surfactants or molecular ligands are commonly used to avoid the aggregation and to control the nanoparticles' shapes [5]. However, these treatments result in unrefined products that require multiple purifications before they can be applied in subsequent nanoparticle processes. This has been deemed to be the adverse effect of chemically synthesized nanoparticles [6], and persisted including in the stabilizations using dendrimer [7] and Polyol [8].

On the other hand, physical syntheses rely on grouping precursors to be made into nanoparticles and involves condensation of vapors, which result from the corresponding physical interactions. Laser becomes one of the most representative physical approaches for synthesis of nanoparticles. An example of laser applications is pulsed laser ablation (PLA) in gas or liquid medium. Invented by Maiman (1960), the technique has become a focal point of more intensive researches. With results differ from the most chemical synthesis methods, PLA offers manufacture of high purity nanoparticles, simpler methods, and mass productions [9]. Simply by permuting the combinations of target solid and choice fluid [10], one can produce a variety of colloidal nanoparticles including metals, alloys, oxides, and semiconductors for many applications including medical applications [11].

In body tissue imaging, one factor responsible for a substance's contrast property is the atomic number, which is described physically by the number of interacting photons. The larger the atomic number means the more photons interact with the atom. In addition, thickness and density also play an important roles in contrast differences [12]. Attenuation coefficient increases accordingly to augmentation of atomic number and density [3]. It greatly affects X-rays attenuation value measured in Hounsfield units (HU).

Silver (Ag; Z = 47), an elastic, easily forged metal, posseses ions which remain neutral under water, acid, and salt environments. Ag shows stability under heat and light [13], and the nanoparticle form has a unique, optical scattering property of plasmon-resonances which allows applications in bio-sensing and imaging [14]. The nano-size bestows it properties to penetrate several biological cell membranes like in bacteria, enhancing the contact surfaces and allowing direct penetration [15]. In this experiment, contrast properties of Silver's Dendrimer Stabilized NPs (DSNPs) in CT Scan were tested. Although Ag's atomic number is relatively low, its DSNPs mode is able to approach the contrast intensity of conventional agents [7]. It is accessible to be produced within reasonable price range as compared to other metals.

Another metal, which is possible to be used as an contrast agent is platinum (Pt; Z = 78), which is often found naturally in alluvium sands throughout various rivers. Owing to its high durability against corrosion, which renders it less toxic than some other metals [16], platinum has been adopted in catalytic modifiers, laboratory equipment, electrical contacts and electrode, resistance thermometers, dentistry equipment, and jewellery. In medicine, the nanoform has shown promises such as in the combination of sinotherapy and radiotherapy, acting simultaneously both as a contrast agent and a drug carrier [17]. A Pt NPs-based contrast agent synthesized in the form of Fe-Pt NPs using Polyol method has also been used in CT Scan. Intravenal injection of the nanoparticles in an animal's tail increased active cells contrast from cancer lesions in scanning for tumor carrier [8]. Comparative study between the use of Pt NPs and commercial iodinate contrast agent has been reported by Anuar et al. [18]. They obtained that the Pt NPs with diameters of 42 nm and 52 nm have higher CT number compared to that of commercial iodinated contrast agents at the same concentration of 1 M. However, still few papers have been reported on Ag and Pt nanoparticles synthesized by using pulse laser ablation for application of contrast agent in CT scan. Researchers generally explore gold nanoparticles functionalized with another material to reduce toxicity. In this present work, we examine a potential Ag and Pt nanoparticles as a candidate of contrast agent in CT scan.

To develop potential candidate of Ag NPs and Pt NPs as contrast agents, this research attempts to look for which NPs among them have best suits for improvement CT Scan imaging. Furthermore, the mixture of Ag and Pt NPs was also examined to know the best suitable candidate for contrast agent in CT scan. The use of PLA method is expected to improve the quality of Ag NPs, Pt NPs, and Ag-Pt NPs as contrast agent, in the hope to find a reliable alternative in CT Scan modalities. Characteristics of Ag-Pt NPs produced in the research was examined using Ultraviolet-Visible Spectroscopy (UV-Vis), Scanning Electron Microscopy (SEM), and X-Ray diffraction (XRD). The produced Ag NPs, Pt NPs, and mixture of Ag-Pt NPs were then applied as a contrast agent via in vitro. The results certified that the colloidal solution having higher concentration of Pt has higher HU value compared to that of Ag NPs, indicating that Pt NPs is better candidate as a contrast agent compared to the Ag NPs case.

Materials and Methods

The pulsed laser ablation method was employed to produce silver (Ag) nanoparticles (NPs), platinum (Pt) nanoparticles (NPs), and a mixture of silver-platinum nanoparticles (Ag-Pt NPs) from the high-purity metal

plates of Ag and Pt (The Nilaco Corporation, Japan), respectively. For synthesis Ag NPs, the decontamination of 99.95%-pure Ag plate with alcohol was followed with incorporation into a petri dish of 25 mL deionized water. To produce a colloidal nanoparticle with a minimum concentration of 20 ppm, the Ag metal plate was bombarded by an Nd: YAG laser beam at a wavelength of 1064 nm with an energy of 45 mJ at a frequency of 10 Hz. During the process, the petri dish was rotated slowly and continuously to obtain a homogeneous nanoparticle fluid. Figure 1 shows the setup of an ablation experiment using a Nd: YAG laser at 1064 nm. In this present work, we used an Nd:YAG laser 1064 nm (New Wave Research Model Polaris II 20 Hz, 7 ns, USA) as an energy source to ablate a material. Some studies on silver nanoparticles synthesis were performed using Nd:YAG laser 1064 nm such as a report by Zamiri et al. [19]. In the study, they produced silver nanoparticles in a virgin coconut oil medium. The result certified that various diameter sizes of nanoparticles are produced depending on laser bombardment time. The averaged sizes are from 4-6 nm, which is applicable for medical applications such as a contrast agent of CT scan.

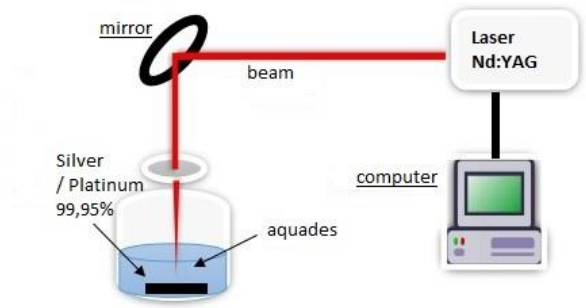

Figure 1. Setup for an Nd: YAG 1064 nm laser ablation experiment

The interaction between the laser and the target was followed with plasma formations resulting in the target's atomic breakdowns. Simultaneous blastsoccurred, followed by shockwave expansions to the surrounding area. With the surrounding temperatures much lower than those of the plasmas, the cooling-downs may result in losses of explosive effects, leaving a mixture of fluid and nanoparticle-sized material referred to as colloidal nanoparticles [20]. The target in the petri dish was moved slowly to avoid a spot being bombarded sequentially, as this affects the quality of nanoparticle formation.

After the treatment of the Ag plate, the laser bombardment was made on the Pt plate using the same method with Ag NPs production. For the Ag-Pt mixture nanoparticles, the experiment was made by following the method described in the paper prepared by Shukri et al. [21]. Namely, the Ag and Pt NPs produced from PLA method were then mixed and stirred into uniformity with variations of compositions: 25:75%, 75:25% and 50:50% of Ag-Pt NPs. The total volume for each composition is 10 ml; e.g., for making a composition of Ag-Pt NPs with mixture composition of 25:75% for Ag-Pt NPs, 2.5 ml colloidal AgNPs (AgNPs concentration of 10 ppm) were mixed with 7.5 ml colloidal PtNPs (PtNPs concentration of 10 ppm). Additional radiation of Nd: YAG 1064 nm laser was applied to the Ag-Pt NPs mixtures for 2 hours laser bombardment to convince that the homogeneous mixture of Ag-Pt NPs was produced.

Sequential tests were performed on the synthesized colloidal Ag NPs, Pt NPs, and Ag-Pt NPs. Using UV-Vis Spectroscopy, the plasma surface resonances were determined, while the NPs' morphology and the average size were derived from the SEM examination. In this present work, we used the SEM method because we only want to analyse the morphology and composition of produced nanoparticles, and we did not study in detail crystal structure and others. These were followed with *X-Ray Diffraction* (XRD) to extract information on the structure type, grid parameters, and different atomic arrangements of the NPs crystals. Analysis on the diameter of the NPs sizes was performed using *Image J* software, which is one of the techniques used for the analysis of nanoparticle diameter [22].

The produced Ag NPs, Pt NPs, and Ag-Pt NPs mixture were examined as a potential contrast agents in CT scans. The CT scan used in this work was commercial CT Philips with a model of ingenuity core 128 and name product of multiscale CT scan 128 slice. This modality has anode effective heat capacity of 30 MHU, anode heat storage capacity of 8 MHU and anode cooling rate of 1,608 KHU/min. This CT is generally used in hospitals in Indonesia. The CT Scan contrast tests began with preparing various mixtures of the NPs into the 10-ml tubesat equal concentrations each and placing them on the holder. In addition, CT Reader software was employed to process the resulting images. Comparative analyses were performed on the HU valuesof the variations. The modality used was Philips multiscale CT scan 128 slices (model of ingenuity core 128, United States). A polystyrene box was placed just on the CT table where the box center is parallel with the gantry isocenter. During the irradiation, the tube voltage and effective current were set at 80 kV and 100 mAs, separately, and the thickness of the slice was 0.6 mm.

Results

The result shown in Figure 2(a) is the dark, brownish-yellow Ag NPs colloid after 13 hours of pulsed-laser bombardment. By contrast, Figure 2(b) shows a clear, brown Pt NPs colloid after10 hours of pulse laserbombardment onthe platinum sample.The shades also indicate the different levels of NPs concentrations: 30 ppm versus 20 ppm, respectively for Ag NPs and Pt NPs colloids. The colloidal concentrations were diluted using deionized water to achieve equalization before CT Scan tests could be performed.

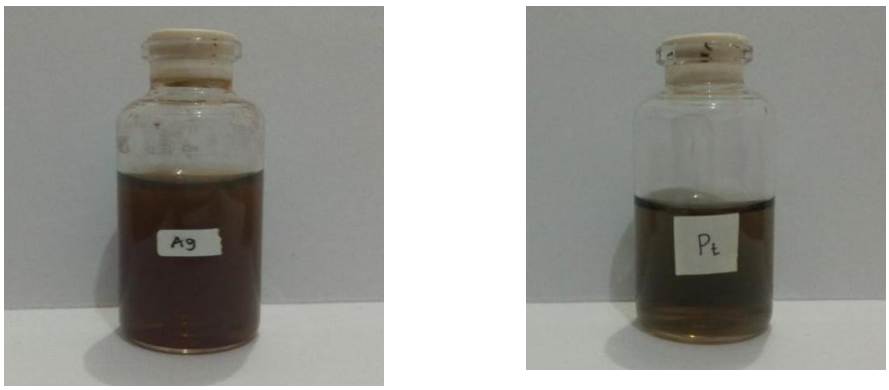

(a) (b)

Figure 2. (a) AgNPs and (b) PtNPs colloids

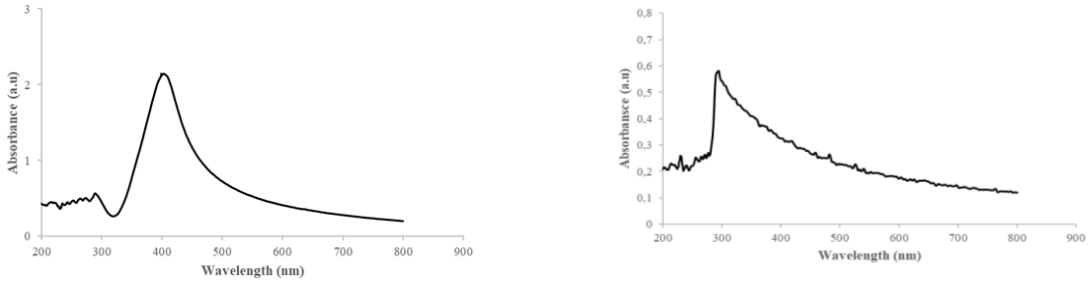

(a) (b)

Figure 3. UV-Vis spectra obtained from(a) colloidalAgNPs and (b) Pt NPs

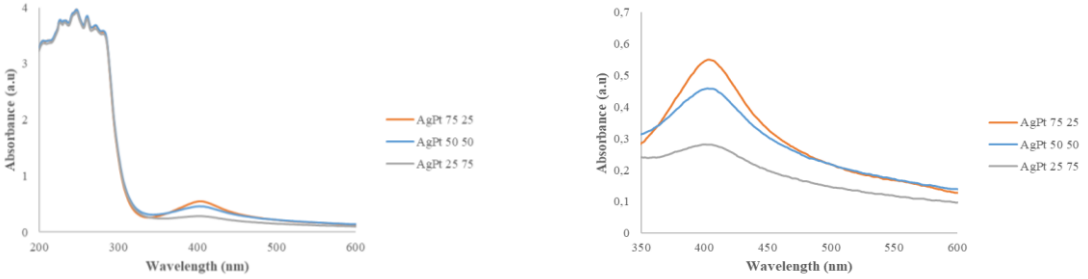

(a) (b)

Figure 4. (a)UV– Visspectraand (b) magnification of the spectra of a mixture of the Ag-Pt NPs colloidal with various volume ratio between Ag and Pt of 75:25% (red curve), 50:50% (blue curve), and 25:75% (grey curve)

To obtain detailed information of produced colloidal Ag and Pt nanoparticles above, characterization of the produced Ag and Pt nanoparticles were further made using Ultraviolet-Visible spectroscopy (UV-Vis), Scanning Electron Microscope (SEM), and X-Ray Diffraction (XRD) methods.

UV-Vis Examination

UV-Vis examines the optical characteristics of the object in terms of absorbance of UV and visible lights wavelengths, in which acquired parameters indicatethe object particlestypes and numbers [13]. First, optical characteristics of pure colloidal Ag and pure colloidal Pt NPs were examined. Figures 3 show UV-Vis absorption spectra obtained from (a) Ag and (b) Pt nanoparticles. It can be seen that for AgNPs, a high absorbance peak of 2.146 arbitrary units occurs at the wavelength of 403 nm. This peak is defined as the peak of localized surface plasmon resonance LSPR, which is an important parameter to identify the type of particles contained in a solution. As is known that silver has an LSPR peak of around 380 nm – 425 nm as reported here [23]. Figure 3(b) specifically confirms the sample as platinum material with an absorbance value of 0.6 a.u. The spectrum shows a structureless broadband extending toward the visible-ultraviolet wavelength range because Pt does not have any wavelength at UV-Vis region. The absorbance spectral image has a similar pattern with the spectrum obtained by Nellore et al [24].

Further study was then made to know the LSPR from the mixture of colloidal Ag-Pt NPs

The absorption peak at the wavelength of around 401-403 nm belongs to AgNPs as reported by Panacek et al. [23]. Therefore, with various concentration of AgNPs in the mixture of Ag-Pt NPs, the absorption intensity of AgNPs vary as shown in Figure 4(b).

XRD Examination

The most frequently used among recent methods for material characterization, X-ray diffraction spectroscopy (XRD) identifies material crystalline phase by parameters specification of the lattice structure and obtains the particle sizesof nanocrystals. It is very handy for studying the crystal structure, chemical composition, and physical properties of nanomaterials [25].

Figure 5 shows the XRD spectra taken from (a) AgNPs, (b) PtNPs, and (d) Ag-Pt NPs. The spectral patterns of AgNPs, PtNPs, and Ag-Pt NPs produced from XRD method of the sample colloids have matched with the data from the previous study [26]. The XRD spectrographs below reveal the elemental and compound existences of the NPs in the colloids. For the Ag sample, the diffraction peaksshowed at 38.0328 (111), 44.2745 (200), and 64.6473 (220) as shown in Figure 5(a), while for the Pt NPs, the diffraction peaks at 33.01 (111) and 66.4 (220) as shown in Figure 5(b). Meanwhile, Ag-Pt NPs sample shows the diffraction peaks at 32.9 (111), 47.6 (200), 67.3 (220) as shown in Figure 5(c). It can be seen in the spectrum that for Ag-Pt NPs mixture, other emission lines of Ag-Pt occurs, which indicated that the Ag-Pt NPs alloys are produced in this present work.

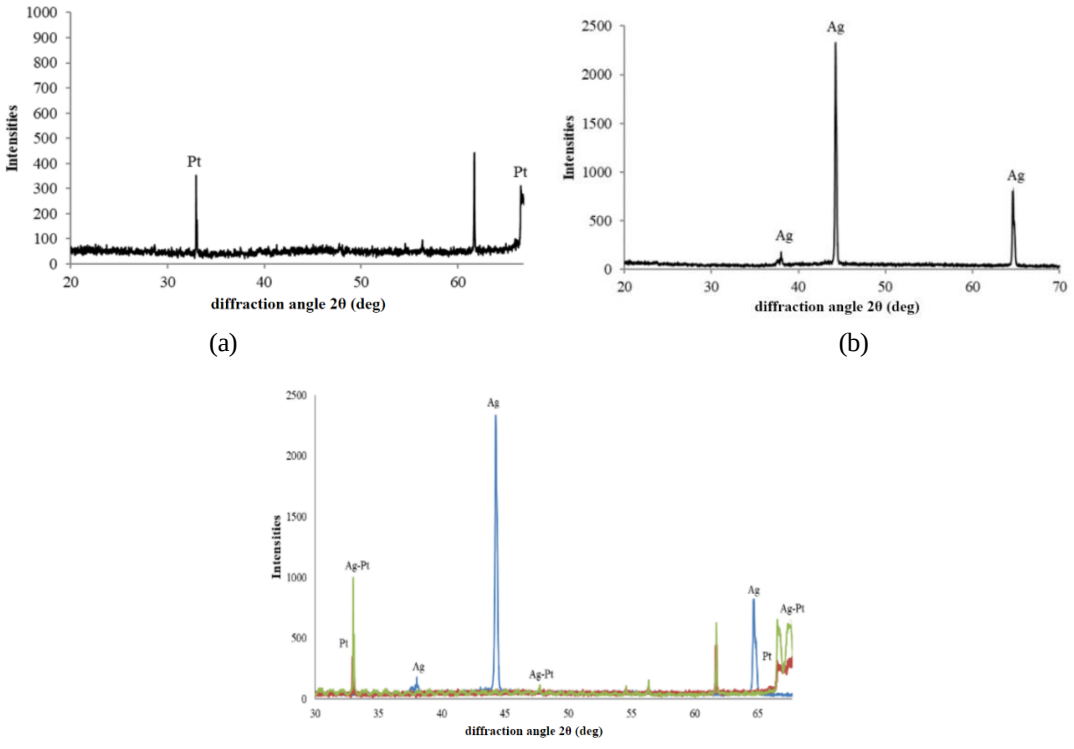

Figure 5. XRD Spectra obtained from (a) AgNPs Sample (b) PtNPs Sample, and (c) Ag-Pt NPs Sample

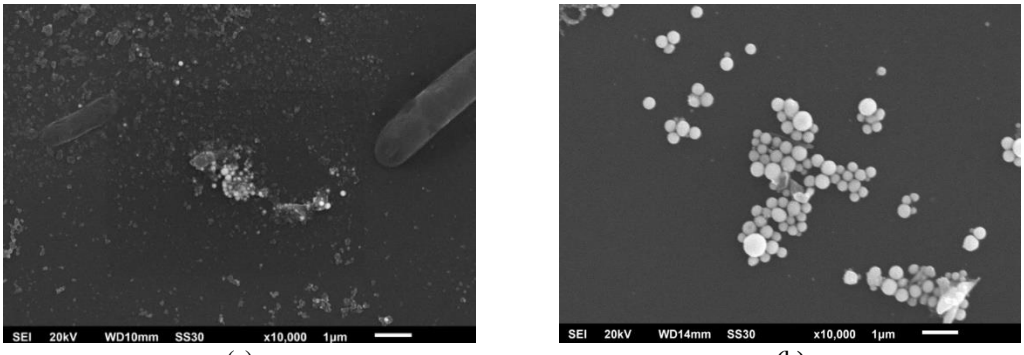

Figure 6. SEM-EDX images obtained from (a) colloidal PtNPs and (b) colloidal AgNPs

SEM Examination

Scanning Electron Microscope (SEM) observed the morphology and determined the size of the NPs. SEM is an efficient method for specimens surfaceimaging. In this study, SEM processing was used with 2000 times magnification. In the case of platinum samples, preparation was performed using colloidal PtNPs produced bypulse laserbombardment at 10 Hz and 45 mJ for repetition rate and laser energy, respectively. A total of 1 ml PtNPs colloid was dripped on ± 0.5x0.5 cm^2 plate of *silica carbide* (SIC), followed by drying with Ovenat 100°C for 30 minutes. Scanning Electron Microscope-Energy Dispersive X-ray (SEM-Energy Dispersive X-ray) result of the colloidal PtNPs is shown in Figure 6 (a).

By using an imageJ processing, the averaged size of PtNPs is 20 nm with a standard deviation of 7 nm, morphologically in the form of brownish spheres as shown in Figure 6(a). Figure 6(b) shows SEM-EDX image from the AgNPs colloid. The AgNPs have a spherical shape. Using an imageJ software, the diameter of AgNPsis estimated to be24 nm with a standard deviation of 5 nm, morphologically in the form of brownish spheres.After achieving colloids of AgNPs and PtNPs, both were homogeneously mixed and synthesized using the pulse laser ablation method at 10 Hz and 45 mJ to obtain a mixture of Ag-Pt NPs. Five variations of colloidal NPs were produced in the experiment with a volume ratio as follows; 100% AgNPs, 75%:25% Ag-PtNPs, 50%:50% Ag-PtNPs, 25%:75% Ag-Pt NPs, and100% PtNPs, each with a concentration of 10 ppm. All of the colloids achieved were inserted into 10ml-sized cylindrical vials.

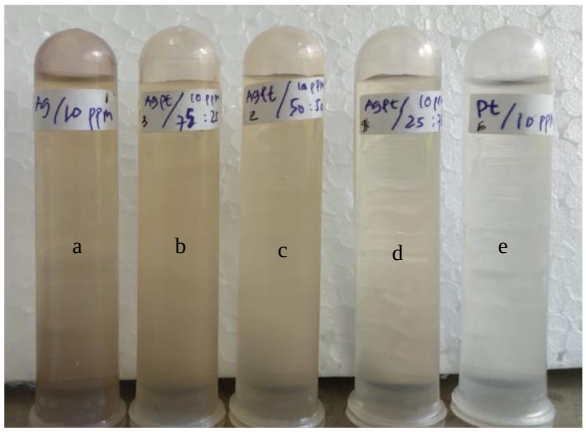

Figure 7.Sample Preparations of (a) 100% AgNPs colloid, (b) 75%:25% Ag-PtNPs colloid, (c) 50%:50% Ag-PtNPs colloid, (d) 25%:75% Ag-PtNPs colloid, and (e) 100% PtNPs colloid in 10ml-sized cylindrical vials

Different shades of the colloids in the tubes imply different NPs compositions. In the left end in Figure 7, the 100% AgNPs colloid has the darkest, brownish-yellow shade, and in the other end, the 100% PtNPs colloid has the most contrastive, transparent, and bright shade. The shadeswere gradually fading and becoming brighter and transparent with the lowering of AgNPs concentration and the raising of PtNPs concentration in the colloid compositions. Hence, the darker the shade means the more AgNPs and the less PtNPs in the composition and, vice versa, the brighter the shade means the fewer AgNPs and the more PtNPs in it. In this phase, colloidal syntheses of AgNPs, PtNPs, and Ag-Pt NPs have been successfully performed and the samples were readily prepared as contrast agents in CT Scan examination.

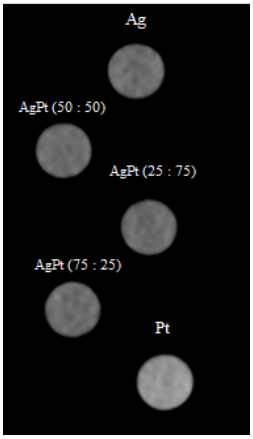

Figure 8. Image results of AgNPs, PtNPs and Ag-PtNPs with variations of compositions as CT Scan contrast agents

The samples were then aligned and scanned by CT-scan simultaneously using a voltage of 80 kV and a current of 100 mAs. The image results depicted in Figure 8 indicate the colloidal NPs' contrast property qualities in HU measurement, represented in the greyish shades. Darker greyish shades represent lower HU values, and vice-versa. The shades are associated with the number of X-ray photons passing through the body tissues which determine the variations of the dark and bright areas in the CT images. The dark areas are called the low-attenuated areas,while the bright areas are the high attenuated [12].

Figure 9 shows HU values of 100% AgNPs, 75%:25% Ag-PtNPs, 50%:50% Ag-PtNPs, 25%:75% Ag-PtNPs, and 100% PtNPs. The CT Scan contrast properties for 100% AgNPs, 75%:25% Ag-PtNPs, 50%:50% Ag-PtNPs, 25%:75% Ag-Pt NPs, and 100% PtNPs colloid were measured by 13.5 HU, 12.8 HU,13.3 HU, 14.1 HU, and 17.3 HU, respectively. This result shows that the 100% PtNPs have the highest CT number is 17.3 HU compared to the case 100% AgNPs and other Ag-Pt NPs mixture with various volume ratios of Ag and Pt with P-value of 0.06. However, it has to be mentioned that the HU values of different NPs reported in this study are not considerably different. As a result, the shades of gray in CT image in Figure 8 are looking similar.

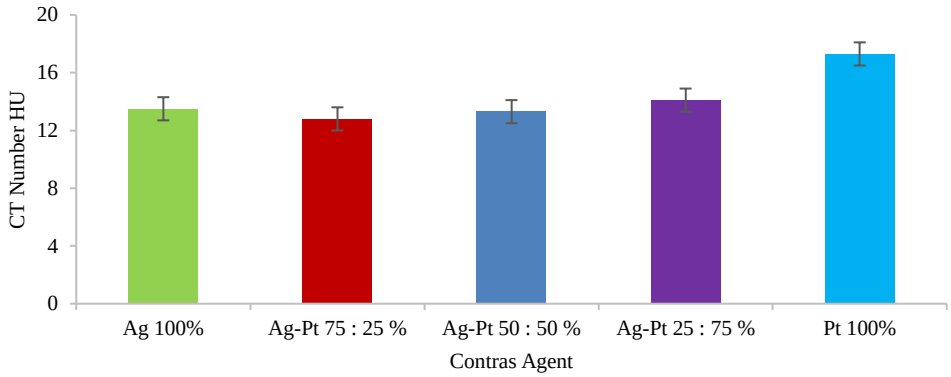

Figure 9. CT Scan tests on contrast properties of 100% AgNPs, 75%:25% Ag-PtNPs, 50%:50% Ag-PtNPs, 25%:75% Ag-Pt NPs, and 100% PtNPs

Discussion

Metal nanoparticles have recently been developed for specific applications of contrast agents in CT scans [3]. This is because nanoparticles have higher absorption than iodine with less bone and tissue interference achieving better contrast with lower X-ray dose. In this present work, we demonstrated the possibility of colloidal AgNPs, PtNPs, and Ag-Pt NPs mixture for contrast agent in CT scan. For this purpose, we have successfully synthesized those nanoparticles by using the pulse laser ablation technique. All colloidal AgNPs, PtNPs, and Ag-Pt NPs have spherical shapes (Figure 6) with averaged diameters of 24 nm and 20 nm for AgNPs and PtNPs, respectively. The produced nanoparticles of AgNPs, PtNPs, and various volume ratios of Ag-Pt NPs mixture were then examined as CT contrast agents.

It is shown in Figure 9 that colloidal PtNPs (PtNPs 100%) gain the highest CT number (HU) is 17.3 HU compared to the case of AgNPs 100% is 13.5 HU and Ag-Pt NPs with various volume ratios with a P-value of 0.06. Also, it should be noticed that the Ag-Pt NPs mixture containing a higher concentration of PtNPs (25%:75% Ag-Pt NPs) has higher CT number compared to the case of Ag-Pt NPs mixture containing higher AgNPs (75%:25% Ag-PtNPs). These findings confirmed that for a colloidal solution containing a high concentration of platinum (PtNPs only and colloidal Ag-Pt NPs mixture with a ratio of 25:75%) has higher x-ray absorbance compared to the case of AgNPs. The higher HU value for Platinium can be attributed to its higher density since the effective energy of 80 kVp (excitation voltage) is about 42 keV, which is much less than the K-edge (binding energy of an electron in K-shell) of Pt (K-edge ≈ 78 keV), which means that the attenuation of X-ray in Pt is due to Compton scattering dominantly.This phenomenon refers to the concept of attenuation coefficient [12], which states high atomic numbers as the one factor responsible for determining better contrasts on scanned tissues. This is explained in physics from the number of photons interacting with a structure, which are influenced by its thickness, density, and atomic numbers. The coefficient of attenuation will increase if the atomic number and density are increased [3]. The coefficient of attenuation greatly affects the attenuation value of X-rays measured in the units of Hounsfield Units (HU). With the NIST data of mass attenuation coefficients indicating 2.6 for silver (Z = 47) and 8.7 for platinum (Z = 78), the results of HU values for the colloidal NPs in this study have been appropriate. As reported by Jakhmola et al., elements with a high atomic number such as gold, silver, platinum, and other heavy metals (Thorium, bismuth, and tantalum) have a high possibility to be employed to enhance the image in CT scan. Lui et al. reported that silver nanoparticles having averaged diameter size of 16 nm displayed X-ray attenuation properties similar to that of iodine-based contrasting agents. For platinum nanoparticles, Chen et al. demonstrated that Pt nanoparticles mixed with Fe can be employed as a dual modal contrast agent of MRI and CT scan. The Pt NPs with averaged sizes ranging from 42-52 nm have higher HU value compared to the case of commercial iodinated contrast agent with the same concentration of 1 mM. In this present work, we used quiet low concentration of 10 ppm for ratio of Ag and Pt nanoparticles with that of water. This comparative study between Ag and Pt was made to evaluate which metal between them is suitable as a contrast agent in CT scan. For next study, we will perform in-vivo study using Ag and Pt nanoparticles with high concentration of around 15-20 times higher than those in this present work as contrast agents in CT scan.

Conclusion

The syntheses of Ag, Pt, and Ag-Pt NPs using pulsed laser ablation technique have been successfully carried out and produced spherical, colloidal nanoparticles (NPs). Comparative analysis among the NPs colloids' shades confirmed the higher AgNPs concentrations to be responsible for darker tones in the colloids, while the higher PtNPs for the brighter.The characteristics of Ag NPs, Pt NPs, and Ag-Pt NPs have been successfully demonstrated by UV Vis spectroscopy,which shows wavelengths of 403 nm and 294 nm respectively for Ag and Pt NPs. In addition, double waves appeared in the imaging graph of colloidal nanoparticle Ag-Pt NPs with wavelength values equal to those of individual UV-Vis

testings of Ag and Pt NPs. The XRD analysis on the synthesized colloidal NPs characteristics confirms the essential NPs compositions in the colloids.In addition, SEM examinations complete the information on the morphology and dimensions of the formed Ag and Pt NPs (each spherical with the average size of 24 nm and 20 nm). Contrast agent testings for the Ag, Pt, and variations of Ag-Pt NPs compositions have been performed *in vitro* in a CT Scan machine, involving five colloidal variations at a concentration of 10 ppm each: 100% AgNPs, 75%:25% Ag-PtNPs, 50%:50% Ag-PtNPs, 25%:75% Ag-Pt NPs, and 100% PtNPs. Results reveal the highest absorbent power was found in the colloidal contrast agent of Pt NPs, followed by the 25:75% Ag-Pt NPs. The higher HU value for Platinum can be attributed to its higher density since the effective energy of 80 kVp (excitation voltage) is about 42 keV, which is much less than the K-edge (binding energy of an electron in K-shell) of Pt (K-edge ≈ 78 keV), which means that the attenuation of X-ray in Pt is due to Compton scattering dominantly.

Acknowledgment

The authors would like to thank to theKarsa Husada Malang Hospitaland the RSUD Loekmono Hadi Kudus for the full support and attention. This study was financially supported by Research Grant from Ministry of Research, Technology, and Higher Education, Indonesia under the contract No. 101-122/UN7.P4.3/PP/2019. Research Grant from Ministry of Research and Technology / BRIN, Indonesia also financially supported part of this study under the contract No.225-135/UN7.6.1/PP/2020.

References

1. Friedland S, Benaron D, Coogan S, Sze DY, Soetikno R. Diagnosis of chronic mesenteric ischemia by visible light spectroscopy during endoscopy. Gastrointestinal Endoscopy, 2007; 65(2): 294-300.
2. Cormode DP, Naha PC, Fayad ZA. Nanoparticle contrast agents for computed tomography: A focus on micelles. Contrast Media and Molecular Imaging. 2014; 9(1): 37–52.
3. Hainfeld JF, Slatkin DN, Focella TM, Smilowitz HM. Gold nanoparticles: A new x-ray contrast agent. British J. Rad. 2006; 79(939): 248–53.
4. Yonezawa T, Toshima N. Bimetallic nanoparticles-novel materials for chemical and physical applications. New J. Chem. 1998; 22(11): 1179–201.
5. Corma A, Garci H. Supported gold nanoparticles as catalysts for organic reactions. Chem. Soc. Reviews. 2008; 37(9): 2096–126.
6. Warner MG, Reed SM, Hutchison JE. Nanoparticles synthesized by interfacial ligand exchange reactions. Chem.Mat. 2000; 12(11): 3316–20.
7. Liu H, Wang H, Guo R, Cao X, Zhao J, Luo Y. Size-controlled synthesis of dendrimer-stabilized silver nanoparticles for x-ray computed tomography imaging applications. Polym. Chem. 2010; 1: 1677–83.
8. Chou S, Shau Y, Wu P, Yang Y. In vitro and in vivo studies of FePt nanoparticles for dual modal CT-MRI molecular imaging. J. Am. Chem. Soc. 2010; 14: 13270–8.
9. Elder A, Yang H, Gwiazda R, Teng X, Thurston SHH. Testing nanomaterials of unknown toxicity: An example based on platinum nanoparticles of different shapes. Adv. Materials. 2007; 19(20): 314–29.
10. Zeng. Nanomaterials via Laser Ablation/Irradiation in Liquid: A Review. Adv. Functional Mat. 2012; 22(7): 1333–53.
11. Amendola V, Meneghetti M, Bakr OM, Riello P, Polizzi S, Anjum DH. Coexistence of plasmonic and magnetic properties in Au 89 Fe 11 nanoalloy. Nanoscale. 2013; 5: 5611–9.
12. Shilo M, Reuveni T, Motiei M, Popovtzer R. Nanoparticles as computed tomography contrast agents: current status and future perspectives. Nanomedicine. 2012; 7(2): 257–69.
13. Dwandaru WSB, Chrishar Putri ZM, Yulianti E. Influence of variation of the concentration of additive material of silver nanoparticles on the Anti-fungal properties of Cat walls as applications of Nano technology in the industrial paint wall. Inotek. 2016; 20: 1-18.
14. Schrand AM, Braydich-Stolle LK, Schlager JJ, Dai L, Hussain SM. Can silver nanoparticles be useful as potential biological labels. Nanotechnology. 2008; 19(23).
15. Navarro E, Piccapietra F, Wagner B, Marconi F, Kaegi R, Odzak N. Toxicity of Silver Nanoparticles to Chlamydomonas Reinhardtii, Env. Scie. Tech. 2008; 42(23):8959–64.
16. World Health Organization. Air quality guidelines for Europe, Copenhagen: World Health Organization, regional office for Europe. Cd Rom. 2000; 2: 1–273.
17. Ferretti V, Bergamini P, Marvelli L, Hushcha Y, Gambari R, Lampronti I. Synthesis and characterization of Pt complexes containing dichloroacetate (DCA), designed for dual anticancer action. Inorg. Chim. Acta. 2018; 470: 119-27.
18. Anuar MAK, Zaky HA, Razak KA, Rahman WN. CT contrast agent of Platinum nanodendrites: Preliminary study. J. Phys.: Conf. Ser. 2019; 1248: 012010.
19. Zamiri R, Azmi BZ, Sadrolhosseini AR, Ahangar HA, Zaidan AW, Mahdi MA. Preparation of silver nanoparticles in virgin coconut oil using laser ablation. Int. J. Nanomed. 2011; 6: 71-5.
20. Dell′Aglio M, Gaudiuso R, Pascale OD, Giacomo AD. Mechanisms and processes of pulsed laser ablation in liquids during nanoparticle production. Appl. Surface Scie. 2015; 348: 4–9.
21. Shukri WNW, Bidin N, Islam S, Krishnan G. Synthesis of Au-Ag alloy nanoparticles in deionized water by pulsed laser ablation technique. J Nanoscie. and Nanotech. 2018; 18: 1-11.

22. Bothun GD. Hydrophobic silver nanoparticles trapped in lipid bilayers: Size distribution, bilayer phase behavior, and optical properties. J. Nanobiotech. 2008; 6(13): 1-10.
23. Panácek A, Kolár M, Vecerová R, Prucek R, Soukupová J, Krystof V, Hamal P, Zboril R, Kvítek L. Antifungal activity of silver nanoparticles against Candida spp. Biomaterials. 2009; 30(31): 6333-40.
24. Nellore J, Pauline C, Amarnath K. Bacopa monnieri phytochemicals mediated synthesis of platinum nanoparticles and its neurorescue effect on 1-methyl 4-phenyl 1,2,3,6 tetrahydropyridine-induced experimental parkinsonism in zebrafish. J. Neurodegenerative Disease. 2013; 1–8.
25. Sharma GD, Mikroyannidis JA, Sharma SS, Justin Thomas KR. Bulk heterojunction organic photovoltaic devices based on small molecules featuring pyrrole and carbazole and 2-(4-nitrophenyl)acrylonitrile acceptor segments as donor and fullerene derivatives as acceptor. Dyes Pigments. 2012; 94: 320–9.
26. Kumar B, Smita K, Cumbal L, Debut A. Synthesis of silver nanoparticles using Sacha inchi (Plukenetia volubilis L.) leaf extracts. Saudi J. Biol. Sci. 2014; 21(6): 605–9.